

## New Methods for Testing Lorentz Invariance with Atomic Systems

R. Shaniv,<sup>1</sup> R. Ozeri,<sup>1</sup> M. S. Safronova,<sup>2,3</sup> S. G. Porsev,<sup>2,4</sup> V. A. Dzuba,<sup>5</sup> V. V. Flambaum,<sup>5</sup> and H. Häffner<sup>6</sup>

<sup>1</sup>*Department of Physics of Complex Systems, Weizmann Institute of Science, Rehovot 7610001, Israel*

<sup>2</sup>*Department of Physics and Astronomy, University of Delaware, Newark, Delaware 19716, USA*

<sup>3</sup>*Joint Quantum Institute, National Institute of Standards and Technology and the University of Maryland, Gaithersburg, Maryland 20742, USA*

<sup>4</sup>*Petersburg Nuclear Physics Institute, National Research Centre “Kurchatov Institute,” Gatchina, Leningrad district 188300, Russia*

<sup>5</sup>*School of Physics, University of New South Wales, Sydney 2052, Australia*

<sup>6</sup>*Department of Physics, University of California, Berkeley, California 94720, USA*



(Received 27 December 2017; published 8 March 2018)

We describe a broadly applicable experimental proposal to search for the violation of local Lorentz invariance (LLI) with atomic systems. The new scheme uses dynamic decoupling and can be implemented in current atomic clock experiments, with both single ions and arrays of neutral atoms. Moreover, the scheme can be performed on systems with no optical transitions, and therefore it is also applicable to highly charged ions which exhibit a particularly high sensitivity to Lorentz invariance violation. We show the results of an experiment measuring the expected signal of this proposal using a two-ion crystal of  $^{88}\text{Sr}^+$  ions. We also carry out a systematic study of the sensitivity of highly charged ions to LLI to identify the best candidates for the LLI tests.

DOI: [10.1103/PhysRevLett.120.103202](https://doi.org/10.1103/PhysRevLett.120.103202)

Local Lorentz invariance (LLI) is a cornerstone of modern physics: The outcome of any local experiment is independent of the velocity and the orientation of the (freely falling) apparatus. The field of Lorentz symmetry tests encompasses almost all fields of physics [1–3] and includes searches for Lorentz violation (LV) in the matter, photon, neutrino, and gravity sectors. While the natural energy scale for strong LV induced by quantum gravity is the Planck scale ( $M_{\text{Pl}} \sim 10^{19} \text{ GeV}/c^2$ ), the consequences of the Lorentz-violating physics may also lead to very small but potentially observable low-energy LV [4,5]. Atomic physics LLI tests were reviewed in Ref. [6]. In this work, we develop new schemes, propose new systems for the LLI tests in the electron-photon sector, performed with either trapped ions or neutral atoms using quantum-information-enabled technologies, and provide proof-of-principle experimental demonstration.

LLI-violating effects are classified in the framework of the standard model extension [3,7]. Violations of Lorentz invariance in bound electronic states result in a small shift of the energy levels described by a Hamiltonian [8]

$$\delta H = - \left( C_0^{(0)} - \frac{2U}{3c^2} c_{00} \right) \frac{\mathbf{p}^2}{2} - \frac{1}{6} C_0^{(2)} T_0^{(2)}, \quad (1)$$

where  $\mathbf{p}$  is the momentum of a bound electron,  $c$  is the speed of light, and  $U$  is the Newtonian gravitational potential. The parameters  $C_0^{(0)}$ ,  $c_{00}$ , and  $C_0^{(2)}$  contain elements of the  $c_{\mu\nu}$  tensor quantifying the LLI violation

[8,9]. The relativistic form of the  $T_0^{(2)}$  operator is  $T_0^{(2)} = c\gamma_0(\boldsymbol{\gamma}\mathbf{p} - 3\gamma_z p_z)$ , where  $\gamma_0$  and  $\boldsymbol{\gamma}$  are the Dirac matrices. The  $c_{\mu\nu}$  tensor has nine components. The  $c_{TJ}$  and  $c_{TT}$  terms describe the dependence of the kinetic energy on the boost of the laboratory frame and have a leading-order time-modulation period related to the sidereal year. The elements  $c_{JK}$ , where  $J, K = X, Y, Z$ , describe the dependence of the kinetic energy on the direction of the momentum and have a leading-order time-modulation period related to the sidereal day (12 and 24 h modulation).

The most sensitive LLI tests for electrons have been conducted with neutral Dy atoms [8] and  $\text{Ca}^+$  ions [9]. Recently, it was proposed to test LLI using a pair of two entangled trapped  $\text{Yb}^+$  ions in the  $4f^{13}6s^2 \ ^2F_{7/2}$  state of  $\text{Yb}^+$  with the prospect to improve the current most stringent bounds by  $10^5$  [10]. However, the proposal of Ref. [10] requires using a decoherence-free subspace to cancel out magnetic field fluctuations. The need to prepare an entangled superposition of two ions leads to three major difficulties: (i) Applying it to the single trapped-ion clock experiments leads to a significant loss of sensitivity, (ii) scaling it to a larger number of ions requires creating a large number of entangled pairs, and (iii) the scheme cannot be readily applied to highly charged ions which often lack strong optical transitions. The scheme proposed here mitigates all these problems without a significant loss of sensitivity and provides a pathway to significantly extend the ultimate accuracy of LLI tests in the electron-photon sector. We also explore a possibility to use highly charged ions or optical-lattice clocks to test the local

Lorentz invariance violation and demonstrate enhancements of the LLI-violating effects in comparison with  $\text{Yb}^+$ .

*Experimental proposal.*—We describe the proposed experimental scheme for the general case and use the example of  $\text{Yb}^+ 2F_{7/2}$  state for modeling. The matrix element of the  $T_0^{(2)}$  operator in Eq. (1) is

$$\langle J, m | T_0^{(2)} | J, m \rangle = \frac{-J(J+1) + 3m^2}{\sqrt{(2J+3)(J+1)(2J+1)J(2J-1)}} \times \langle J || T^{(2)} || J \rangle, \quad (2)$$

where  $J$  and  $m$  denote the quantum numbers of the total electronic angular momentum and its projection on the quantization axis, respectively. Therefore, the tensor LLI-violating signal contains a term proportional to  $m^2$ . Thus, the experimental goal is to monitor the splitting between different  $m$  levels as Earth rotates around its axis and around the Sun and, thus, place a bound on  $C_0^{(2)}$ . Typically, the main source of decoherence in this type of experiment is the magnetic field noise leading to uncontrolled Zeeman shifts. In order to reduce the effect of magnetic field noise while maintaining the  $m^2$ -dependent effects, we propose a dynamical decoupling (DD) [11] technique that is applicable to spins of an arbitrary size.

*General physical system description.*—We consider a spin  $J$  system whose associated magnetic moment  $\mu_z$  interacts with a magnetic field:  $\mathbf{B} = B_z \hat{\mathbf{z}}$ . The Hamiltonian  $\mathcal{H}_{\text{lin}} = \mu_z B_z J_z$  has equidistant energy eigenstates  $|J, m\rangle$ . In addition to this linear Zeeman effect, we assume a small energy shift proportional to  $m^2$ , which can result from possible Lorentz-violating terms but also from a second-order Zeeman shift or the electric quadrupole shift originating in ion traps from their inherent electric field gradient. This shift enters the Hamiltonian as  $\mathcal{H}_{\text{quad}} = \kappa J_z^2$ . The total free evolution Hamiltonian is the sum of linear and quadratic terms  $\mathcal{H}_{\text{free}} = \mathcal{H}_{\text{quad}} + \mathcal{H}_{\text{lin}} = \kappa J_z^2 + \mu_z B_z J_z$ . We assume that we can drive our system with a radio-frequency (rf) oscillating magnetic field tuned close to the resonance transition frequency  $\omega_{\text{rf}} = (\mu_z B_z / \hbar) + \delta(t)$ , where  $\delta(t)$  accounts for drifts in the ambient magnetic field at the spin's position. This drive translates to adding the time-dependent coupling term  $\mathcal{H}_{\text{coup}} = \Omega(t) \cos(\omega_{\text{rf}} t + \phi) J_x$  to the Hamiltonian, where  $\Omega$  is the multilevel Rabi frequency and  $\phi$  is the rf phase. Moving to the interaction picture with respect to the oscillating magnetic field and applying the rotating wave approximation, we obtain the evolution Hamiltonian:

$$\mathcal{H} = \delta(t) J_z + \kappa J_z^2 + \Omega(t) [J_x \cos(\phi) - J_y \sin(\phi)]. \quad (3)$$

In what follows, we assume that  $\Omega(t)$  can take values of  $\Omega_0 \gg \kappa, \delta(t)$  and 0. According to Eq. (3), that means that while applying a rf drive with duration  $\sim (\pi/\Omega_0)$  the evolution due to

$\mathcal{H}_{\text{free}}$  can be neglected, while the evolution due to  $\Omega_0 [J_x \cos(\phi) - J_y \sin(\phi)]$  is significant.

*Experimental scheme.*—In the following, we describe the DD method aimed at measuring  $\kappa$  while mitigating the unwanted magnetic field noise  $\delta(t)$  by a periodic modulation of  $\Omega$  and  $\phi$ . This method is premised on a scheme published in Ref. [12], where it was used to measure the electric quadrupole shift, and is in a sense a generalization of the ubiquitous spin-echoed Ramsey sequence for a large spin  $J$ . For clarity, we describe a specific DD sequence, although other types of DD sequences may be applied as well. The sequence begins with initializing our spin state in a specific  $J_z$  eigenstate  $|J, m = m'\rangle$ . A resonant rf pulse is then applied for a duration of  $\tau = (\pi/2\Omega_0)$  ( $\pi/2$  pulse). We define the phase of this pulse to be  $\phi = 0$ , and therefore the corresponding evolution operator is  $\exp[i(\pi/2)J_x]$ . This pulse maps the spin state to the corresponding  $J_y$  eigenstate and, thus, acts as the first  $\pi/2$  pulse of a Ramsey sequence. Next, a modulation sequence is applied, in the form of

$$[t_w] - [\pi_{+y}] - [2t_w] - [\pi_{-y}] - [t_w],$$

where  $\pi_{\pm y}$  are rf pulses with duration  $\pi/\Omega_0$  ( $\pi$  pulses) with  $\phi = \pm(\pi/2)$  and  $2t_w$  is the wait time between pulses, where the spin evolves freely. We choose the time  $t_w$  such that over  $4t_w$  time  $\delta(t)$  changes slowly and is effectively constant. Therefore, we can write the evolution of the spin system as

$$\begin{aligned} \mathcal{U} &= \exp(i[\delta t_w J_z + \kappa t_w J_z^2]) \\ &\times \exp(-i\pi J_y) \exp(i[2\delta t_w J_z + 2\kappa t_w J_z^2]) \exp(i\pi J_y) \\ &\times \exp(i[\delta t_w J_z + \kappa t_w J_z^2]). \end{aligned} \quad (4)$$

As a result of the commutation relation  $[J_z^2, \exp(\pm i\pi J_y)] = 0$ , the signal term  $\kappa J_z^2$  generates a phase shift, which is coherently accumulated during the sequence. However,  $[J_z, \exp(\pm i\pi J_y)] \neq 0$ , and thus the phase due to the magnetic noise term  $\delta(t)J_z$  is largely reduced by averaging. The evolution operator then reads  $\mathcal{U} = \exp(i4\kappa t_w J_z^2)$ .

Following  $n$  repetitions of  $\mathcal{U}$ , a second  $\pi/2$  pulse is applied, with a rf phase  $\phi$  with respect to the first  $\pi/2$  pulse. The evolution of the entire sequence, after a total time of  $T = 4nt_w$ , can be written as

$$\begin{aligned} \mathcal{U}_{\text{total}} &= \exp\left(\frac{\pi}{2} [J_x \cos(\phi) - J_y \sin(\phi)]\right) \\ &\times \exp(i\kappa T J_z^2) \exp\left(\frac{\pi}{2} J_x\right). \end{aligned} \quad (5)$$

Finally, the population in the initial state  $|J, m = m'\rangle$ ,  $P_{J, m'}(\kappa T, \phi) = |\langle J, m' | \mathcal{U}_{\text{total}} | J, m' \rangle|^2$ , is measured. Since  $T$ , the total experiment time, is known and  $\phi$  can be calibrated,  $P_{J, m'}(\kappa T, \phi)$  can be directly used to estimate  $\kappa$ .  $P_{J, m}(\kappa T, \phi)$  is therefore an equivalent of the Ramsey fringe in this

large- $J$  Ramsey-sequence generalization. The theoretical calculation of  $P_{J,m}(\kappa T, \phi)$  for  $J = \frac{7}{2}$  and  $m = -\frac{7}{2}, -\frac{1}{2}$  are shown in Fig. 1. By repeating this measurement sequentially in time and recording  $P_{J,m}(\kappa T, \phi)$ ,  $\kappa$  can be extracted. Figures 1(c) and 1(d) show the expected signal as a function of  $\kappa T$  for  $\phi = 0$ . The proposed experiment consists of monitoring the results of sequential measurements in time of  $P_{J,m}(\kappa T, \phi)$  and looking for a time-dependent variation at the theoretical sidereal day and sidereal year periods. An optimal point to search for variations in  $\kappa$  would be around the point at which  $P_{J,m}(\kappa T, \phi = 0)$  has the steepest slope with respect to  $\kappa T$ , indicated by the red dashed lines in Figs. 1(a) and 1(b). See Supplemental Material [13] for further discussion. Experimentally, it will be likely easiest to choose the total Ramsey time  $T$  to maximize the slope, but also the trap frequency and magnetic field can be used to tune  $\kappa$  via the electric quadrupole or second-order Zeeman shifts.

Notice that this method contains only local spin operations. It is therefore straightforward to generalize this method for an ensemble of  $N$  spins, e.g., a large ion chain or neutral atoms in an optical lattice. The uncertainty in evaluating  $\kappa$  thus reduces by a factor of  $\sqrt{N}$ .

In addition, our procedure requires only initializing and detecting one specific state:  $|J, m\rangle$ . This is useful in systems where logic spectroscopy [16] must be used, e.g., for highly charged trapped ions. Moreover, even if weak optical

transitions are required to initialize and read out the final state, the coherent operations are carried out with rf only, thus avoiding effects from systematic ac-Stark shifts.

Another advantage of the rf-manipulation scheme is that the wavelength of the rf radiation is much longer than the motional amplitudes of the ions, allowing for high-fidelity coherent manipulation even at high temperatures. While one may still require optical fields to initialize and read out the states, stimulated Raman adiabatic passage or sequentially repeated pulses can be used, yielding high state transfer fidelities even if the quality of a  $\pi$  pulse would be low [17]. Finally, we note that one can also use strong rf field gradients to drive sideband transitions. As a consequence, one can apply quantum logic spectroscopy and detect the state of probe ions even if there are no optical transitions available opening up the possibility to use any highly charged ion (HCI) whose ground state has an angular moment of larger than  $2\hbar$ .

*Measurement sensitivity.*—One important aspect is how sensitive the presented method is as compared to the method presented in Ref. [10]. The contribution of Lorenz violation effects to  $\kappa$  is given by Eq. (2):

$$\kappa_{\text{LLI}}/2\pi = 5.1 \times 10^{15} \text{ Hz} \times C_0^{(2)}. \quad (6)$$

In Supplemental Material [13], we evaluate the measurement precision  $\Delta\kappa$  with which  $\kappa$  can be measured for  $J = \frac{7}{2}$ . We find that it is optimal to use  $m = \frac{1}{2}$  as an initial state and estimate for this case  $\Delta\kappa = 0.1(\text{rad}/\sqrt{N\tau T})$ , where  $T$ ,  $\tau$ , and  $N$  are the interrogation time, total integration time, and the number of spin probes, respectively. For comparison,  $\Delta\kappa$  calculated for the method presented in Ref. [10] is  $\Delta\kappa = 0.083(\text{rad}/N\sqrt{\tau T})$ . While for small ion or atom numbers  $N$  both methods yield similar precisions, the method presented here can be readily extended to larger  $N$ , while the method in Ref. [10] is more difficult to scale due to the complexity in exploiting quantum correlations.

*Proof-of-principle experimental demonstration.*—In order to verify the scheme, we measured  $\kappa$  for the  $4D_{5/2}$  level in two  $^{88}\text{Sr}^+$  ion chains trapped in a linear Paul trap [13]. The dominant contribution to  $\kappa$  comes from the quadrupole shift, which can be used as a resource to tune our system to the most sensitive measurement point. We initialized our ions in the  $m = -\frac{3}{2}$  and implemented the above DD sequence for times between  $600 \mu\text{s}$  and  $33 \text{ ms}$ , with up to 110 pulses using  $t_w = 150 \mu\text{s}$ . The results along with the corresponding theoretical expectations are presented in Fig. 2.

*Neutral atoms in optical lattices.*—Our DD scheme can also be applied to neutral atoms which allow for a large number  $N$  of probes and have already been successfully employed for LLI tests in electromagnetic sector [8]. To overcome systematic effects, it may be advantageous to trap them in optical lattices where potentially  $10^5$  or more atoms may be held in the future [18]. In the current lattice clocks,

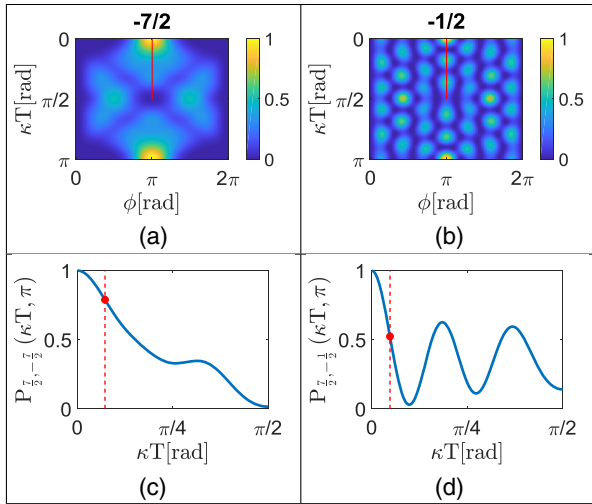


FIG. 1. Theoretical calculation of  $P_{7/2,m}(\kappa T, \phi)$  for different  $m$  values.  $P_{7/2,m}$  is periodic in  $\kappa T$  with a period of  $\pi$ , and it is symmetric with respect to  $\pm m$ . Therefore, we plot only negative  $m$  values and  $\kappa T \in [0, \pi]$ . (a),(b) Theoretical calculation of  $P_{7/2,-7/2}(\kappa T, \phi)$ ,  $P_{7/2,-1/2}(\kappa T, \phi)$  as a function of  $\phi$  and  $\kappa T$ , respectively. The solid red line marks the  $\phi = \pi$  line, where the Ramsey fringe should be measured for maximal sensitivity. (c),(d) Ramsey fringe in the  $m = -\frac{7}{2}, -\frac{1}{2}$ , respectively, as a function of  $\kappa T$ . The curves correspond to the populations along the red solid lines in the (a) and (b) plots, respectively. The red dashed line marks the highest sensitivity  $\kappa T$ , and the red full circle marks the corresponding value of  $P_{J,m}(\kappa T, \phi)$ .

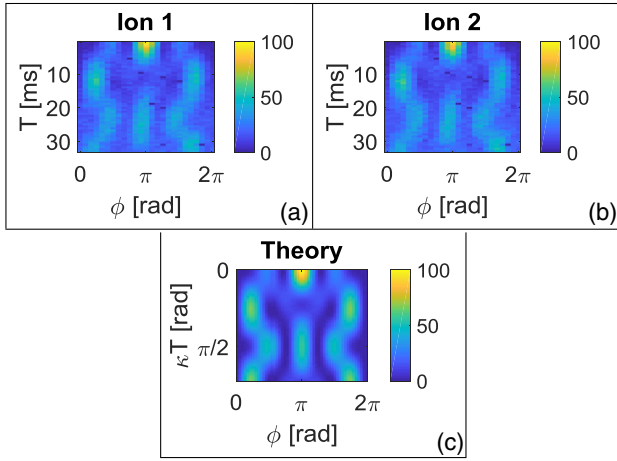


FIG. 2. Experimental verification of the DD method on the  $4D_{5/2}$  level of two trapped  $^{88}\text{Sr}^+$  ions. (a),(b) The measurement of  $P_{5/2,-3/2}(\kappa T, \phi)$  in percent after the above DD sequence for different  $T$  and  $\phi$ , for ion 1 and ion 2, respectively. In the experiment,  $t_w = 150 \mu\text{s}$  and the DD pulse number goes from 2 to 110 (see Supplemental Material [13]). (c) The theoretical calculation of  $P_{5/2,-3/2}(\kappa T, \phi)$ .

such as Sr, Yb, or Mg,  $J = 0$  states are used, exhibiting no sensitivity to tensor LLI in the electromagnetic sector. Nevertheless, other precision LLI tests could be possible with neutral atom clocks, such as, for example, measuring LLI effects due to the first term in Eq. (1) and measuring  $c_{\mu\nu}$  in the nucleon sector using isotopes with nuclear spin  $I > 1/2$ ; see [19–22]. For the LLI tests in the electron sector with neutral atoms, the ground state of Tm, having the same electronic  $4f^{13}6s^2 2F_{7/2}$  configuration as  $\text{Yb}^+$ , appears to be rather well suited, as it has the same high sensitivity as  $\text{Yb}^+$ . Moreover, Tm is already being pursued for lattice clock development, and trapping of the ensemble of Tm atoms in a 1D optical lattice has been demonstrated [23]. We note that a Tm clock is not needed for an LLI test, just the ability to perform the scheme described here for the Tm ground state. Using Yb, the metastable  $4f^{13}5d6s^2 J = 2$  state could be used, too. For neutral atoms held in optical lattices, an additional systematic effect may arise from the trapping beams due to ac-Stark shifts of the Zeeman components.

*Highly charged ions.*—A number of HCIs were recently shown to be candidates for the development of atomic clocks and the search for variation of the fine-structure constant  $\alpha$  [24,25]. Experimentally, the sympathetic cooling of a HCI was demonstrated in Ref. [26] for  $\text{Ar}^{13+}$ , and the spectra of an  $\text{Ir}^{17+}$  ion, suitable for the above applications, were explored in Ref. [27]. We have carried out the calculation of the matrix elements of the  $T_0^{(2)}$  operator in the wide range of HCIs and find an enhancement in the LLI effects for the states containing 1–2 valence electrons or holes in the  $nf$  shell. HCIs have a number of important advantages: (i) The LLI probe state is a ground state in many ions, allowing for the straightforward application of

the scheme, (ii) there is a wide variety of the ions to choose from, and (iii) there is an extra enhancement factor with the degree of ionization.

The calculations for the monovalent ions are carried out using the linearized coupled-cluster single-double method (see [28] for a review). The calculation for the other ions are carried out using a method combining a configuration interaction with a modified linearized single-double coupled-cluster approach [29,30]. The details of the calculations are described in Supplemental Material [31]. The results for selected HCIs are summarized in Table I. We list only the HCIs where LLI can be tested in the ground state, since it simplifies the implementation scheme as it requires only a logic ion and rf pulses. The calculations are carried out for the ions already suggested for the design of atomic clocks and tests of  $\alpha$  variation [25,36–39]. The table lists the reduced matrix elements  $|\langle J || T^{(2)} || J \rangle|$  (in a.u.) and LLI-induced energy shift (in hertz) between the highest and lowest values of the magnetic quantum numbers  $|m_J|$ , for example,  $m_J = 7/2$  and  $m_J = 1/2$  for  $J = 7/2$ . The  $\text{Ca}^+$  and  $\text{Yb}^+$  values are listed for reference. We list the number of electrons  $N$  for convenience. With the exception of the case with  $N = 58$ , we list only the ions of the isoelectronic sequence with the lowest ionization charges which have at least one  $nf$  electron in the ground state. More highly charged ions from the same isoelectronic sequence can be

TABLE I. The reduced matrix elements  $|\langle J || T^{(2)} || J \rangle|$  (in a.u.) and LLI-induced energy shift (in hertz) between the highest and lowest values of  $|m|$ . The  $\text{Ca}^+$ ,  $\text{Yb}^+$ , and  $\text{Yb}$  values are for the excited states; all other values are for the ground states.  $N$  is the number of electrons in an ion.

Ion	$N$	Level	$J$	$ \langle J    T^{(2)}    J \rangle $	$ \Delta E / (hC_0^{(2)}) $
$\text{Ca}^+$	19	$3d$	$5/2$	9.3	$4.5 \times 10^{15}$ [9]
$\text{Yb}^+$	69	$4f^{13}6s^2$	$7/2$	135	$6.1 \times 10^{16}$ [10]
Tm	69	$4f^{13}6s^2$	$7/2$	141	$6.4 \times 10^{16}$
Yb	70	$4f^{13}5d6s^2$	2	74	$3.9 \times 10^{16}$
$\text{Th}^{3+}$	87	$5f$	$5/2$	47	$2.2 \times 10^{16}$
$\text{Sm}^{15+}$	47	$4f$	$5/2$	128	$5.7 \times 10^{16}$
$\text{Sm}^{14+}$	48	$4f^2$	4	124	$5.5 \times 10^{16}$
$\text{Sm}^{13+}$	49	$5s^2 4f$	$5/2$	120	$5.8 \times 10^{16}$
$\text{Eu}^{14+}$	49	$4f^2 5s$	$7/2$	120	$5.4 \times 10^{16}$
$\text{Nd}^{10+}$	50	$4f^2$	4	96	$4.3 \times 10^{16}$
$\text{Cf}^{15+}$	83	$5f 6p^2$	$5/2$	112	$5.4 \times 10^{16}$
$\text{Cf}^{17+}$	81	$5f$	$5/2$	144	$6.9 \times 10^{16}$
$\text{Os}^{18+}$	58	$4f^{12}$	6	367	$1.4 \times 10^{17}$
$\text{Pt}^{20+}$	58	$4f^{12}$	6	412	$1.6 \times 10^{17}$
$\text{Hg}^{22+}$	58	$4f^{12}$	6	459	$1.8 \times 10^{17}$
$\text{Pb}^{24+}$	58	$4f^{12}$	6	507	$2.0 \times 10^{17}$
$\text{Bi}^{25+}$	58	$4f^{12}$	6	532	$2.1 \times 10^{17}$
$\text{U}^{34+}$	58	$4f^{12}$	6	769	$3.0 \times 10^{17}$

used as well and are expected to have even larger sensitivities to LLI. We demonstrate this point in the lower part of the table, where we list a number of ions with 58 electrons and the same  $4f^{12}$  ground state configurations but with an increasing ionization charge.  $\text{Bi}^{25+}$ , which can be produced with a small tabletop electron-beam ion traps, already has factor of 4 larger matrix element in comparison with  $\text{Yb}^+$ . The enhancement with the ionization charge occurs for all other isoelectronic sequences as well, so a very large number of HCIs are suitable for the LLI tests using the experimental scheme describe above. We also list  $\text{Th}^{3+}$ , since it can be directly laser cooled [40] and has a  $5f_{5/2}$  ground state. It can serve as an excellent experiment test bed for later experiments with HCIs.

In summary, we proposed an experimental scheme for a drastic improvement of the LLI tests in the electron sector. The scheme is applicable to any atomic spin system, including single and highly charged trapped ions and neutral atomic lattice clocks. It does not involve correlating operations between different spin probes, which simplifies the experimental procedure to a large extent.

This work was supported in part by NSF Grant No. PHY-1620687 (USA) and No. PHY-1507160 (USA). The UNSW group acknowledges support by the Australian Research Council. R. S. and R. O. acknowledge support by the ICore-Israeli excellence center circle of light, the Israeli Ministry of Science Technology and Space, the Minerva Stiftung and the European Research Council (consolidator Grant 616919-Ionology). M. S. S. thanks the School of Physics at UNSW, Sydney, Australia for hospitality and acknowledges support from the Gordon Godfrey Fellowship program, UNSW. S. G. P. acknowledges support from Russian Foundation for Basic Research under Grant No. 17-02-00216.

---

[1] D. Mattingly, *Living Rev. Relativity* **8**, 5 (2005).  
 [2] S. Liberati and L. Maccione, *Annu. Rev. Nucl. Part. Sci.* **59**, 245 (2009).  
 [3] V. A. Kostelecký and N. Russell, *Rev. Mod. Phys.* **83**, 11 (2011).  
 [4] V. A. Kostelecký, *Phys. Rev. D* **69**, 105009 (2004).  
 [5] C. M. Will, *Living Rev. Relativity* **17**, 4 (2014).  
 [6] M. S. Safronova, D. Budker, D. DeMille, D. F. J. Kimball, A. Derevianko, and C. W. Clark, *arXiv:1710.01833*.  
 [7] D. Colladay and V. A. Kostelecký, *Phys. Rev. D* **58**, 116002 (1998).  
 [8] M. A. Hohensee, N. Leefler, D. Budker, C. Harabati, V. A. Dzuba, and V. V. Flambaum, *Phys. Rev. Lett.* **111**, 050401 (2013).  
 [9] T. Pruttivarasin, M. Ramm, S. G. Porsev, I. Tupitsyn, M. S. Safronova, M. A. Hohensee, and H. Häffner, *Nature (London)* **517**, 592 (2015).  
 [10] V. A. Dzuba, V. V. Flambaum, M. S. Safronova, S. G. Porsev, T. Pruttivarasin, M. A. Hohensee, and H. Häffner, *Nat. Phys.* **12**, 465 (2016).

[11] D. A. Lidar and T. A. Brun, *Quantum Error Correction* (Cambridge University Press, Cambridge, England, 2013).  
 [12] R. Shaniv, N. Akerman, and R. Ozeri, *Phys. Rev. Lett.* **116**, 140801 (2016).  
 [13] See Supplemental Material at <http://link.aps.org/supplemental/10.1103/PhysRevLett.120.103202> and Refs. [14,15] for detailed description of the experimental system.  
 [14] D. J. Wineland, C. Monroe, W. M. Itano, D. Leibfried, B. E. King, and D. M. Meekhof, *J. Res. Natl. Inst. Stand. Technol.* **103**, 259 (1998).  
 [15] N. Akerman, N. Navon, S. Kotler, Y. Glickman, and R. Ozeri, *New J. Phys.* **17**, 113060 (2015).  
 [16] P. O. Schmidt, T. Rosenband, C. Langer, W. M. Itano, J. C. Bergquist, and D. J. Wineland, *Science* **309**, 749 (2005).  
 [17] D. B. Hume, T. Rosenband, and D. J. Wineland, *Phys. Rev. Lett.* **99**, 120502 (2007).  
 [18] S. L. Campbell, R. B. Hutson, G. E. Marti, A. Goban, N. Darkwah Oppong, R. L. McNally, L. Sonderhouse, J. M. Robinson, W. Zhang, B. J. Bloom, and J. Ye, *Science* **358**, 90 (2017).  
 [19] P. Wolf, F. Chapelet, S. Bize, and A. Clairon, *Phys. Rev. Lett.* **96**, 060801 (2006).  
 [20] M. Smiciklas, J. M. Brown, L. W. Cheuk, S. J. Smullin, and M. V. Romalis, *Phys. Rev. Lett.* **107**, 171604 (2011).  
 [21] H. Pihan-Le Bars, C. Guerlin, R.-D. Lasserri, J.-P. Ebran, Q. G. Bailey, S. Bize, E. Khan, and P. Wolf, *Phys. Rev. D* **95**, 075026 (2017).  
 [22] V. V. Flambaum and M. V. Romalis, *Phys. Rev. Lett.* **118**, 142501 (2017).  
 [23] D. Sukachev, S. Fedorov, I. Tolstikhina, D. Tregubov, E. Kalganova, G. Vishnyakova, A. Golovizin, N. Kolachevsky, K. Khabarova, and V. Sorokin, *Phys. Rev. A* **94**, 022512 (2016).  
 [24] J. C. Berengut, V. A. Dzuba, and V. V. Flambaum, *Phys. Rev. Lett.* **105**, 120801 (2010).  
 [25] M. S. Safronova, V. A. Dzuba, V. V. Flambaum, U. I. Safronova, S. G. Porsev, and M. G. Kozlov, *Phys. Rev. Lett.* **113**, 030801 (2014).  
 [26] L. Schmöger, O. O. Versolato, M. Schwarz, M. Kohnen, A. Windberger, B. Piest, S. Feuchtenbeiner, J. Pedregosa-Gutierrez, T. Leopold, P. Micke, A. K. Hansen, T. M. Baumann, M. Drewsen, J. Ullrich, P. O. Schmidt, and J. R. C. López-Urrutia, *Science* **347**, 1233 (2015).  
 [27] A. Windberger, J. R. Crespo López-Urrutia, H. Bekker, N. S. Oreshkina, J. C. Berengut, V. Bock, A. Borschevsky, V. A. Dzuba, E. Eliav, Z. Harman, U. Kaldor, S. Kaul, U. I. Safronova, V. V. Flambaum, C. H. Keitel, P. O. Schmidt, J. Ullrich, and O. O. Versolato, *Phys. Rev. Lett.* **114**, 150801 (2015).  
 [28] M. S. Safronova and W. R. Johnson, *Adv. At. Mol. Opt. Phys.* **55**, 191 (2008).  
 [29] M. G. Kozlov, *Int. J. Quantum Chem.* **100**, 336 (2004).  
 [30] M. S. Safronova, M. G. Kozlov, W. R. Johnson, and D. Jiang, *Phys. Rev. A* **80**, 012516 (2009).  
 [31] See Supplemental Material at <http://link.aps.org/supplemental/10.1103/PhysRevLett.120.103202> and Refs. [32–35] for a description of the theoretical methods.

- [32] S. A. Blundell, W. R. Johnson, Z. W. Liu, and J. Sapirstein, *Phys. Rev. A* **40**, 2233 (1989).
- [33] S. A. Kotochigova and I. I. Tupitsyn, *J. Phys. B* **20**, 4759 (1987).
- [34] V. A. Dzuba, V. V. Flambaum, and M. G. Kozlov, *Phys. Rev. A* **54**, 3948 (1996).
- [35] V. A. Dzuba, J. C. Berengut, C. Harabati, and V. V. Flambaum, *Phys. Rev. A* **95**, 012503 (2017).
- [36] V. A. Dzuba, A. Derevianko, and V. V. Flambaum, *Phys. Rev. A* **86**, 054501 (2012).
- [37] M. S. Safronova, V. A. Dzuba, V. V. Flambaum, U. I. Safronova, S. G. Porsev, and M. G. Kozlov, *Phys. Rev. A* **90**, 042513 (2014).
- [38] M. S. Safronova, V. A. Dzuba, V. V. Flambaum, U. I. Safronova, S. G. Porsev, and M. G. Kozlov, *Phys. Rev. A* **90**, 052509 (2014).
- [39] V. A. Dzuba, M. S. Safronova, U. I. Safronova, and V. V. Flambaum, *Phys. Rev. A* **92**, 060502 (2015).
- [40] C. J. Campbell, A. G. Radnaev, and A. Kuzmich, *Phys. Rev. Lett.* **106**, 223001 (2011).